

## ORIGINAL RESEARCH

## Sustainable Energy

# Thermal and combustion characteristics of honge, jatropha, and honge-jatropha mixed biodiesels

Vinay Atgur<sup>1</sup> | G. Manavendra<sup>2</sup> | B. Nageswara Rao<sup>1</sup> | Ibham Veza<sup>3</sup> |  
I. M. Rizwanul Fattah<sup>4</sup> 

<sup>1</sup>Department of Mechanical Engineering, Koneru Lakshmaiah Education Foundation (KLEF), K L Deemed to be University, Green Fields, Guntur, India

<sup>2</sup>Department of Mechanical Engineering, Bapuji Institute of Engineering and Technology (BIET), Davangere, India

<sup>3</sup>Faculty of Mechanical Engineering, Universiti Teknikal Malaysia Melaka, Melaka, Malaysia

<sup>4</sup>Centre for Technology in Water and Wastewater (CTWW), School of Civil and Environmental Engineering, Faculty of Engineering and IT, University of Technology Sydney, Ultimo, New South Wales, Australia

## Correspondence

Vinay Atgur, Department of Mechanical Engineering, Koneru Lakshmaiah Education Foundation (KLEF), K L Deemed to be University, Green Fields, Vaddeswaram, Guntur, Andhra Pradesh 522502, India.  
Email: [atgurvinay@gmail.com](mailto:atgurvinay@gmail.com)

I. M. Rizwanul Fattah, Centre for Technology in Water and Wastewater (CTWW), School of Civil and Environmental Engineering, Faculty of Engineering and IT, University of Technology Sydney, Ultimo, 2007 New South Wales, Australia.  
Email: [islammdrizwanul.fattah@uts.edu.au](mailto:islammdrizwanul.fattah@uts.edu.au)

## Funding information

University of Technology Sydney,  
Grant/Award Number: 2200034

## Abstract

Thermal characteristics of biodiesels are useful in system design, modeling, and operation. Such investigations are extensively being carried out in combustors, engine, and process industries. This article examines the thermal characteristics of jatropha (*Jatropha curcas*), honge (*Pongamia pinnata*), and their equal mixing from thermogravimetry and differential scanning calorimetry (TG-DSC) curves for the specific 10°C/min heating rate under atmospheric air. Fuel properties are measured following ASTM standards to compare with diesel properties. Each experiment was repeated three times, and the properties showed insignificant scatter. The average properties of the repeated tests are presented. Two phases of decomposition were observed for diesel, whereas three (viz., devolatilization of aqueous fractions, combustion of methyl esters, and combustion of carbonaceous residues) in biodiesels. Jatropha oil methyl ester (JOME) is thermally stable compared to honge oil methyl ester (HOME). Mixed biodiesel (JOME+HOME) is prone to oxidation due to the high content of oleic and linoleic acids. Recorded onset and offset temperatures of mixed biodiesel are low compared to pure biodiesel. Mixed biodiesel exhibited high volatility resembling diesel characteristics. It exhibited an enthalpy of 240 J/g, whereas the enthalpy of diesel, jatropha, and honge exhibited enthalpies of 130, 321, and 570 J/g, respectively. The combustion index (*S*) of diesel, jatropha, honge, and mixed biodiesel was 41.6, 82.8, 77.74, and 64.6, respectively. Mixed biodiesel reduces the intensity of combustion ( $H_p$ ), promising better combustion characteristics. Thus, mixed biodiesel shows the potential of an efficient alternative energy source.

## KEYWORDS

biodiesel, combustion, degradation, honge, jatropha, mixed biodiesel

## 1 | INTRODUCTION

The world is currently experiencing a scarcity of fossil fuels and environmental degradation due to the extensive consumption of these

fuels. Fossil fuel consumption reduces subterranean carbon capacity, necessitating the development of alternative energy sources that can meet our daily needs.<sup>1</sup> Electric power generation, motor vehicles, and aviation operations are gradually transitioning to biodiesel utilization.<sup>2,3</sup>

This is an open access article under the terms of the [Creative Commons Attribution-NonCommercial](https://creativecommons.org/licenses/by-nc/4.0/) License, which permits use, distribution and reproduction in any medium, provided the original work is properly cited and is not used for commercial purposes.

© 2023 The Authors. *Environmental Progress & Sustainable Energy* published by Wiley Periodicals LLC on behalf of American Institute of Chemical Engineers.

Transesterification is used to produce these oxygenated fuels.<sup>4,5</sup> Alcohols convert triglycerides into glycerol, methyl esters, or ethyl esters, depending on which alcohol is used.<sup>6</sup> To conduct an analysis of combustion chemistry, it is essential to investigate the recurring patterns of reactions that occur during combustion.<sup>7–9</sup> The knowledge of fuel oxidation and decomposition of esters is crucial in understanding the combustion mechanism of biodiesels.<sup>10</sup> During combustion, nitrogen in the air and/or fuel combines with oxygen to generate NO<sub>x</sub>, which can eventually produce nitric acid vapor after interacting with ammonia, moisture, and other components in the atmosphere.<sup>11–13</sup> Furthermore, the combustion of fuels increases greenhouse gases such as CO, CO<sub>2</sub>, PM, SO<sub>x</sub>, and so forth.<sup>14–16</sup> The storage of biofuels causes them to degrade, necessitating a stability analysis of the fatty acid profiles of feedstock.<sup>17–19</sup> In the primary oxidation process, the carbon atom of methylene between olefin atoms strikes first.<sup>20</sup> Close to the double bond, the methylene carbon atom affects the oxidation rate.<sup>21</sup> When hydroperoxides break down and interact during the reaction, the secondary oxidation products form.<sup>22</sup> These secondary oxidation products are aldehydes, alcohols, high molecular weight polymers, and carboxylic acids.<sup>23</sup>

Many biomass resources, such as agricultural, forestry, municipal solids, and industrial wastes, can be used as solid fuels or converted to gaseous fuels to generate energy via thermal conversion processes such as combustion, torrefaction, gasification, and pyrolysis, among others.<sup>24–26</sup> Thermal characteristics must be thoroughly understood before these procedures can be improved. For example, El-Sayed et al.<sup>27</sup> utilized thermogravimetric/differential thermogravimetric (TG/DTG) analysis to investigate the thermal breakdown and oxidation, combustion properties, and kinetics of cotton stalks and sugarcane bagasse powder of various particle sizes in the air at different heating rates from room temperature to 1000°C. They reported that all of the samples demonstrated a two-stage response mechanism between 200 and 1000°C, showing areas of volatile oxidation and char combustion during thermal degradation and oxidation. Kotaiah Naik et al.<sup>28</sup> studied the torrefaction and kinetics of deoiled Karanja seed cake as an upgrading method for this feedstock. They reported that the reduction in O/C and H/C caused a considerable shift in elemental composition, boosting the calorific value, and hydrophobicity of the torrefied biomass. According to the kinetics investigation, a single-step reaction mechanism was sufficient to characterize the overall kinetics of the torrefaction process and explain the thermochemical phenomena.

Jatropha and honge (with nearly 40% of the oil content in the kernel) are abundantly available.<sup>25,29</sup> These non-edible feedstocks are ideal for biodiesel production. Combustion simulations necessitate advanced computing capabilities as well as a thorough understanding of chemical kinetics.<sup>30</sup> So far, most researchers have concentrated on coal combustion phenomena, with very few studies done on liquid fuels, particularly biodiesel combustion analysis. Atgur et al.<sup>31</sup> recently reviewed the literature on Thermogravimetry analysis (TGA) and differential scanning calorimetry (DSC) to analyze heat flow, enthalpy, and thermal stability. They reported that the B20 blend has a high enthalpy, higher thermal stability, and a lower combustion peak

temperature, as well as an enhanced combustion index and combustion intensity that is virtually similar to diesel. Atgur et al.<sup>32</sup> studied the thermal behavior of diesel, *Jatropha curcas* biodiesel, and its 20% blend in diesel. They suggested that due to the higher temperature combustion of the stable intermediate compounds that are formed, the peak combustion temperature is higher for jatropha oil methyl ester (JOME) compared to diesel and B20 blends. Volli and Purkait<sup>33</sup> examined the thermo-chemical characteristics of mustard, soybean, olive, and Karanja oils by conducting TG-DTG experiments in a nitrogen atmosphere up to 600°C with heating rates of 10–100°C/min and observed a single stage of decomposition. The high activation energy was noticed in Karanja, followed by soybean, mustard, and olive oils. Farias et al.<sup>34</sup> examined the thermal stability of biodiesel blends in 20% passion fruit, 20% castor oil biodiesel, and 20% biodiesel blend of passion fruit and castor oil. TG curve indicated high stability of castor oil biodiesel. Oleic and linoleic acids in passion fruits lead to low thermal stability due to high oxidation. Blends of passion fruit and castor oil biodiesel (1:1 proportions) indicated high thermal stability. Increased stability in 1:2 proportions is due to the ricinoleic acid content in castor oil. Santos et al.<sup>35</sup> investigated the thermal stability and physicochemical properties of biodiesels produced from cotton, sunflower, palm oil, and their B-10 blends. TG curve of palm oil indicated high initial decomposition temperature and two-mass loss steps, whereas single mass loss for sunflower and cotton oils. The high onset temperature of cotton oil biodiesel indicated high thermal stability and also, observed high decomposition temperature of blends.

Dwivedi and Sharma<sup>36</sup> observed long storage deterioration of the oxidation and thermal stability of Pongamia biodiesel. Thermal degradation of the samples followed the first-order reaction the addition of antioxidant PY increased the induction period and activation energy. Conceição et al.<sup>37</sup> observed the thermal degradation of castor oil biodiesel at 150–210°C in a synthetic air atmosphere exposing up to 48 h. Mass loss (%), peak temperature, and enthalpy with temperature presented at 10°C/min heating rate. Castor biodiesel stability was noticed up to 150°C and formed intermediate compounds at high temperatures. John et al.<sup>38</sup> generated fuel properties by adopting spectrometric methods (like GC-MS and Fourier transform infrared spectrum [FTIR] with thermogravimetry and differential scanning calorimetry [TG-DSC]) to assess the quality of hemp (*Cannabis sativa* L.) biodiesel. DSC and TG-DTG results matched well with GC-MS and FTIR results. Wnorowska et al.<sup>39</sup> examined halloysite additives on fuels to generate TG-DTG profiles and analyzed the combustion profiles.

The thermal characteristics of a specific fuel can be used to explain the performance and emissions of a CI engine powered by that fuel. Banapurmath et al.<sup>40</sup> examined the CI engine's performance and emissions operating on jatropha, honge, and sesame methyl esters (JOME, HOME, and SOME). Brake thermal efficiency (BTE) for honge oil methyl ester (HOME), SOME, and JOME at 80% load was reported as 29.51%, 30.4%, and 29%, respectively (whereas 31.25% BTE for diesel). Ignition delay enhancement was observed with combustion duration. SOME and HOME showed improvement in heat release rate. JOME and HOME showed low unburnt hydrocarbon (HC) and

**TABLE 1** Properties of diesel and biodiesels.

Fuel	Calorific value (MJ/kg)	Kinematic viscosity @40°C (cSt)	Cetane value	Density (kg/m <sup>3</sup> )	Flash point (°C)	Pour point (°C)	Cloud point (°C)
Diesel	44.22	2.87	47.8	840	76	−3	6.5
HOME	38.66	4.92	51	870	140	4.3	13.2
JOME	39.79	4.73	52	862.2	182.5	3	3
JOME+HOME	40	4.805	52	870.8	142	2	12

carbon monoxide (CO) emissions. In their study, Deepanraj et al.<sup>41</sup> investigated the combustion characteristics of blends comprising 20% jatropha and Karanja biodiesel with diesel. The experiments were conducted using a single-cylinder diesel engine operating at a speed of 1500 rpm. At full load, the thermal efficiency of 29.8%, 29%, and 28.6% were reported for diesel, 20% jatropha biodiesel blend in diesel, and 20% Karanja biodiesel blend in diesel. Soudagar et al.<sup>42</sup> studied *Moringa oleifera* based B10 and B20 blends performance and emission characteristics at full load conditions with engine speeds varying from 1000 to 2400 rpm. They reported increased CO (2.5%) and NO<sub>x</sub> (9%) emissions compared to diesel for B10.

Until now, the primary focus of researchers has been to investigate coal combustion phenomena, with relatively fewer studies on liquid fuels, particularly in the area of biodiesel combustion analysis. Conventional engine testing methods have limitations in that they only provide performance indicators and lack insight into the thermodynamic aspects. However, by employing TGA and DSC techniques, it is possible to assess the combustion behavior of liquid fuels and enhance their storage conditions. These studies can also facilitate the optimization of fuel blends before subjecting them to engine testing, thus, reducing the need for extensive engine bench tests. Motivated by the investigations of the above researchers, this paper examines thermal and combustion characteristics of JOME, HOME, and combined honge-jatropha biodiesel at equal proportions performing TG-DSC experiments using NETZSCH 449F3 simultaneous thermal analyzer for 10°C/min heating rate in atmospheric air. Evaluated combustion index (*S*) and intensity of combustion (*H<sub>i</sub>*) using DTG curves and reported the peak combustion temperature, enthalpy, onset-offset temperature, stability, ignition, and burnout temperature.

## 2 | MATERIALS AND METHODS

Biodiesels of Jatropha oil and honge oil are prepared through a transesterification process. HOME and JOME procured from the University of Agriculture Sciences (Gandhi Krishi Vigyana Kendra–GKVK, Bangalore). Equally mixed biodiesel (JOME+HOME) blends were prepared and placed in a beaker. Initially, homogenized for 15 min by a magnetic stirrer and 20 min with an ultrasonicator. Viscosity, specific gravity, flash point, and calorific value of JOME, HOME, and mixed biodiesel were determined as per the ASTM-D6751 standards. The heating value of blends was obtained using a bomb calorimeter, whereas density was measured using a hydrometer at 30°C.

The Redwood viscometer was used for kinematic viscosity at 40°C. Pensky–Martens apparatus used for the flash and fire points 40–250°C. A wax appearance test was performed to obtain the cloud point. The properties of diesel and biodiesels are compared in Table 1.

FTIR is used for examining compounds formed by the transesterification of jatropha and honge oil and biodiesel blend characteristics. Biodiesels contain fatty acid methyl esters (FAMES) with a carbonyl group. The infrared spectrums were recorded in 3000–700 cm<sup>−1</sup>. TG-DSC experiments were performed (with 10°C/min heating rate from atmospheric temperature to 500°C) in the air using NETZSCH Make simultaneous thermal analyzer- STA 449F3. Samples were analyzed in an alumina crucible pan, performing T-zero calibration as well as enthalpy/temperature calibration. Weight change with temperature plots is referred to as thermogravimetric curves or thermograms. Figures 1 and 2 show the schematic of the TG-DSC system and equipment.

Combustion characteristics of biodiesels examined in air. TG-DTG curve in Figure 3 depicts stages of combustion and ignition temperature, *T<sub>i</sub>* (which is the intersection of tangent lines at the beginning and at *T<sub>max</sub>*). At burnout temperature (*T<sub>b</sub>*), 98% of conversion (*α*) occurs at a single stage of the combustion process.

The conversion (*α*) at *T* is

$$\alpha_T = \frac{w_0 - w_T}{w_0 - w_f} \times 100\%. \quad (1)$$

Here, *w<sub>0</sub>* and *w<sub>f</sub>* are weights at the beginning and end of combustion. *w<sub>T</sub>* is the weight at *T*.

The ignition index (*D<sub>i</sub>*) and burnout index (*D<sub>b</sub>*) are:

$$D_i = \frac{DTG_{max}}{T_{max} \times T_i}, \quad (2)$$

$$D_b = \frac{DTG_{max}}{\Delta T_{0.5} \times T_{max} \times T_i}. \quad (3)$$

Here,  $\Delta T_{0.5}$  is half the peak width of the DTG curve.

The combustion index (*S*) is:

$$S = \frac{DTG_{max} \times DTG_{mean}}{T_b \times T_i^2}. \quad (4)$$

Here,

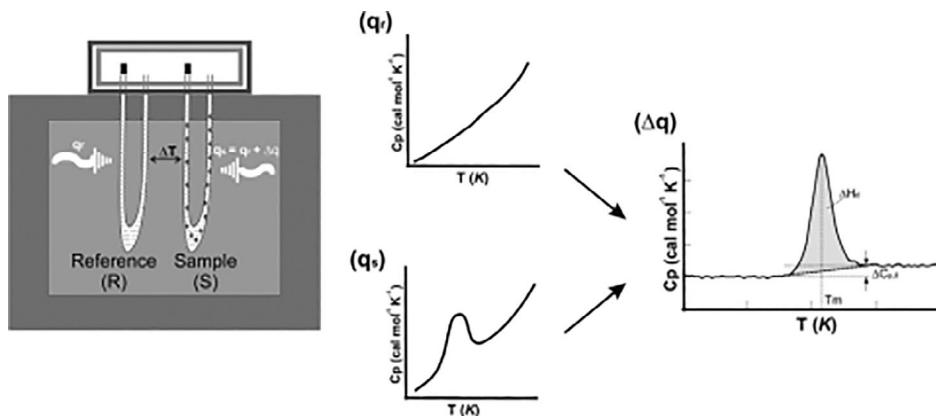


**FIGURE 1** Schematic representation of TG-DSC experimental system.

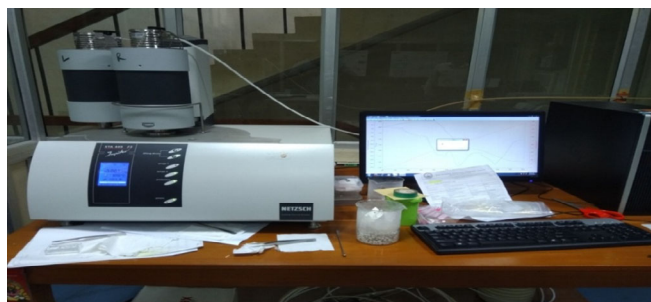


**FIGURE 2** TG-DSC instrument makes NETZSCH STA 449F3.

$$DTG_{\text{mean}} = \frac{\beta(\alpha T_b - \alpha T_i)}{(T_b - T_i)}, \quad (5)$$

and  $\beta$  is the heating rate. The combustion index ( $S$ ) measures a fuel's ignition, combustion, and burnout properties.<sup>43</sup>

The intensity of combustion ( $H_f$ ) is:

$$H_f = T_{\text{max}} \times \ln\left(\frac{\Delta T_{0.5}}{DTG_{\text{max}}}\right) \times 10^{-3}. \quad (6)$$

A high value of the Ignition index ( $D_i$ ) and burnout index ( $D_b$ ) and a low value of the intensity of combustion ( $H_f$ ) represent faster reactions between fuel and air/oxygen and therefore, higher energy release rate and better combustion rate.

### 3 | RESULTS AND DISCUSSION

FTIR spectroscopy for HOME and JOME showed in Figures 4 and 5. Stretching vibration resulted in two strong bands related to symmetric and asymmetric vibrations of C—H stretching at 2923 and 2853  $\text{cm}^{-1}$ . The band at 1741  $\text{cm}^{-1}$  indicated little variation in stretching vibration due to the carbonyl group (—C=O). The bending vibration of the  $\text{CH}_2$  and  $\text{CH}_3$  groups showed variations in strong peaks at 1435  $\text{cm}^{-1}$ . Due to wagging vibrations of the  $\text{CH}_2$  group, HOME and JOME had strong peaks at 1168  $\text{cm}^{-1}$ .<sup>44</sup> The peak at 722  $\text{cm}^{-1}$  indicated rocking vibrations of =C—H groups.

FTIR spectra in Figure 6 showed equally mixed JOME and HOME biodiesel. Strong bands of symmetric and asymmetric vibrations of C—H stretching resulted at 2923 and 2853  $\text{cm}^{-1}$ . A strong band at 1742  $\text{cm}^{-1}$  indicated stretching vibration due to the carbonyl group. Bending vibrations of  $\text{CH}_2$  and  $\text{CH}_3$  groups showed strong peaks at 1436  $\text{cm}^{-1}$ . Due to the wagging vibrations of the  $\text{CH}_2$  group, the mixed biodiesel had a strong peak at 1169  $\text{cm}^{-1}$ . A peak at 722  $\text{cm}^{-1}$  indicated the rocking vibrations of =C—H groups.

In the combustion phenomenon, HCs exhibited exothermic reactions. DSC curve of diesel exhibited endothermic reaction at 37–96°C. In the endothermic region (evaporation zone), lighter fractions of diesel heated up and occurred endothermic cracking reaction.<sup>45</sup> Maximum combustion temperature attained at 251.4°C with an enthalpy of 130.4 J/g. Diesel consists of  $\text{C}_5$ – $\text{C}_{12}$  with a boiling range of 190–375°C. High heat release with a premixed burning phase during diesel combustion resulted in high thermal efficiency. HOME, JOME, and mixed biodiesels exhibited endothermic processes up to 119, 53, and 47°C. The peak temperature of combustion for HOME, JOME, and mixed biodiesel are 294, 292.1, and 287.5°C, respectively. Compared to diesel, biodiesel combustion rapidly occurs due to oxygen content.<sup>46</sup> High Cetane number of biodiesels leads to a short delay in time, subsequently, more time taken to complete combustion. Similar results have been observed by Mohammed et al.<sup>47</sup> The range of Carbon numbers in HOME, JOME, and mixed biodiesels are  $\text{C}_{14}$ – $\text{C}_{20}$ ,  $\text{C}_{12}$ – $\text{C}_{20}$ , and  $\text{C}_{12}$ – $\text{C}_{18}$ . The absence of arachidic and behenic acids in mixed biodiesel reduced combustion duration and interval compared to pure biodiesel. These obtained results are in line with those of Chabane et al.<sup>48</sup> and Nicolas et al.<sup>49</sup> Figure 7 shows a comparison of DSC combustion curves. Table 2 gives the reaction region temperature, peak combustion temperature, heat flow, and enthalpy.

Diesel molecules have different lengths and properties. Thermal degradation of diesel takes place in two phases. The oxidation of lighter compounds takes place in the initial stage, followed by the formation of peroxides and other incomplete combustion products. This behavior has been previously observed by Freire et al.<sup>50</sup> in the case of Jatropha oil. Diesel degradation takes place from 45 to 498°C within 47.7 min. Olefins, paraffin, naphthenes, and aromatics decompose from 119 to 260°C.<sup>51</sup> JOME is thermally stable up to 145°C. JOME degradation takes place from 145 to 334°C. Key fatty acid

**FIGURE 3** Stages of combustion in a typical TG-DTG curve.

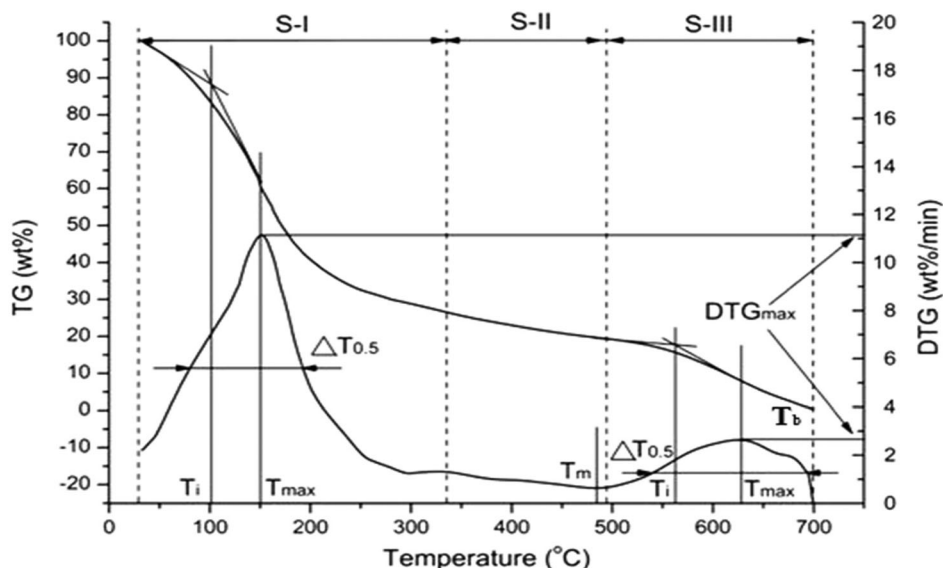


**FIGURE 4** FTIR spectroscopy of HOME.

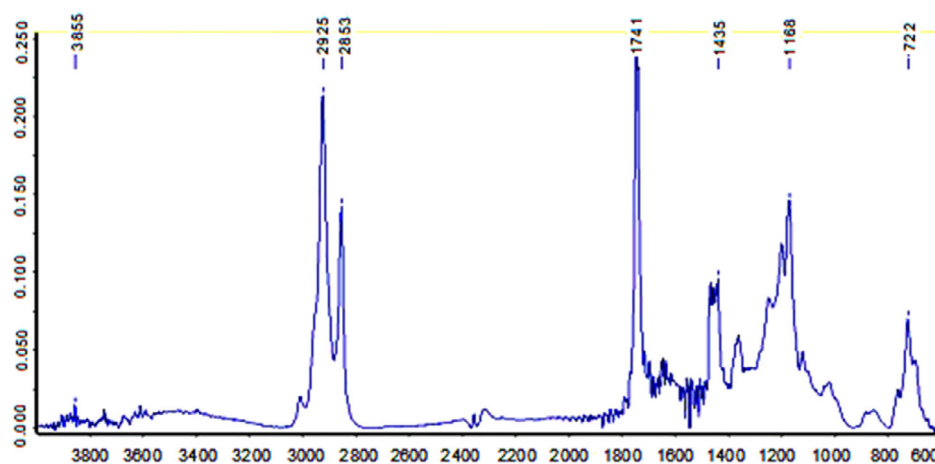
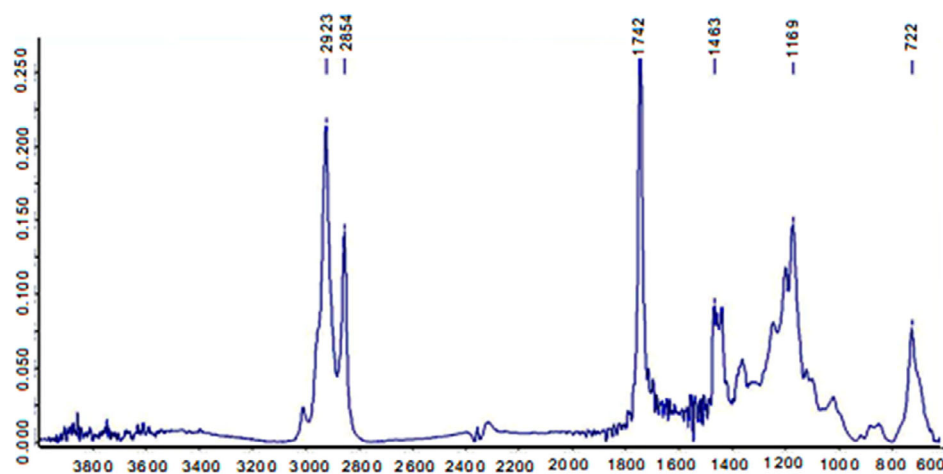


**FIGURE 5** FTIR spectroscopy of JOME.



components in JOME are 49% oleic acid, 22.5% palmitic acid, 12% linolenic acid, and 5.5% stearic acid.<sup>52</sup> HOME is thermally stable up to 150°C because of fatty acid content. Degradation of HOME takes place rapidly beyond 210°C with steep curves up to 297°C.

The majority of the fatty acids in HOME are linoleic, oleic, and palmitic acids (having decomposition temperatures of 240, 270, and 353°C). Fatty acids like stearic, behenic, and linolenic degrade above 300°C. Mixed biodiesel is thermally stable up to 167°C with an offset

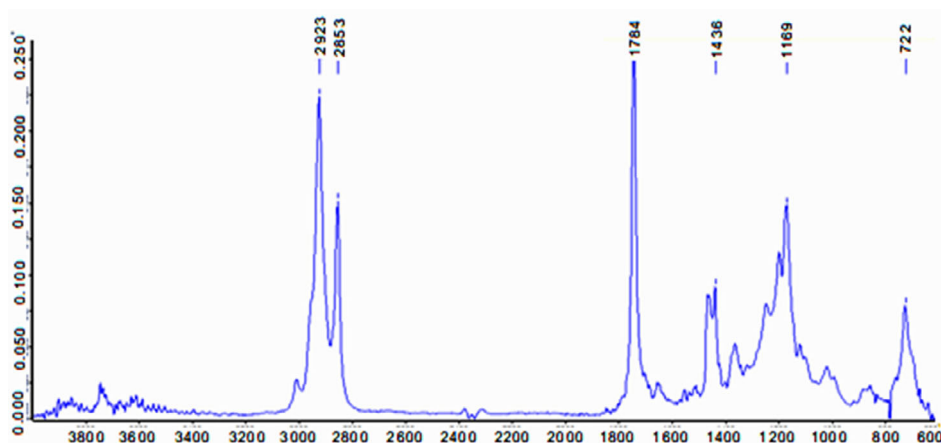


**FIGURE 6** FTIR spectra of equally mixed JOME and HOME biodiesel.

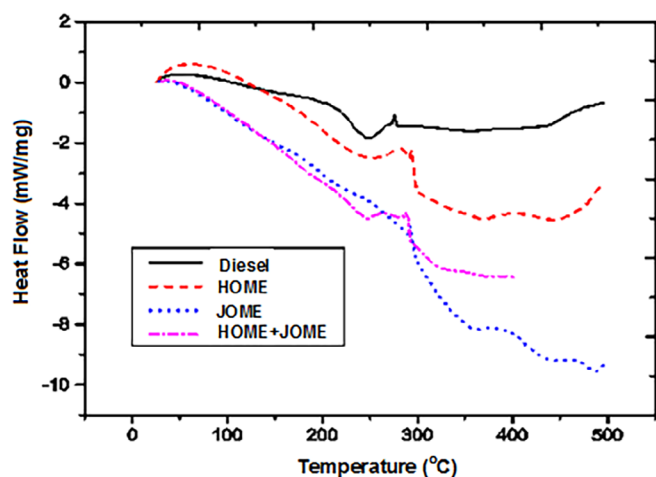


**FIGURE 7** Comparison of DSC combustion curves.

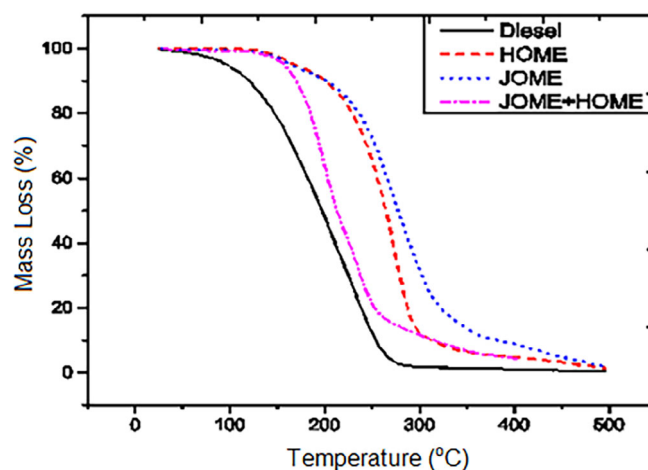


**FIGURE 8** Comparison of TG curves for different fuels.

**TABLE 2** Heat flow and enthalpy at peak temperature.

Sample	Reaction region temperature (°C)	Peak temperature (°C)	Heat flow (mW/mg)	Enthalpy (J/g)
DIESEL	34–270	251.4	−1.851	130.4
HOME	119–442	294	−2.21	570
JOME	43–435	292.1	−4.727	321
JOME+HOME	42–390	247.7, 287.5	−4.512	240

temperature of 267°C. Compared to HOME and JOME, mixed biodiesel exhibited low reaction temperatures, indicating a faster rate of burning within a shorter time interval. Three steps of decomposition were observed for biodiesels: evaporation of methyl esters; decomposition of mono, di, and triglycerides; and high carbon fatty acids (like oleic, linoleic, and palmitic). These results are in accordance with the previous studies of Jain and Sharma<sup>53</sup> and Soto et al.<sup>54</sup> Degradation in the third step involves carbonization with minimum mass loss (3%), decomposing alcoholic esters, fatty acids, and degradation residues in the previous phase. The high viscosity of biodiesels leads to a slow

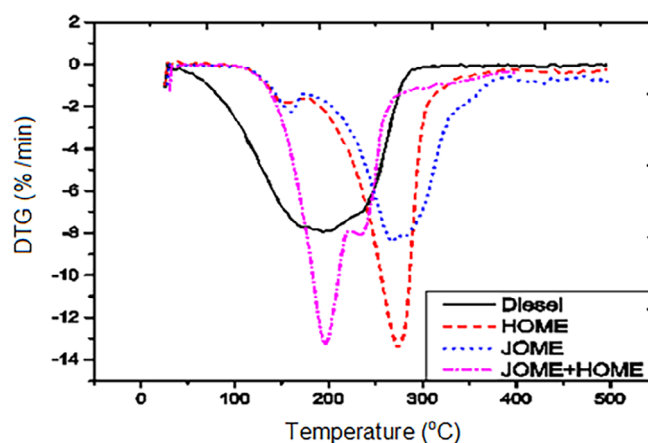


**FIGURE 9** Comparison of DTG curves for different fuels.

evaporation process and high thermal stability as illustrated by Peer et al.<sup>55</sup>

TG profiles with temperature are in descending order due to the volatilization of weak chemical bonds, molecular absorption, and buoyancy. Figures 8 and 9 show TG and DTG curves for HOME,

**TABLE 3** Onset, offset, reaction region, and maximum temperature of biodiesels.

Sample	Onset temperature, $T_e$ (°C)	Offset temperature, $T_o$ (°C)	Reaction region temperature (°C)	Maximum decomposition temperature, $T_{max}$ (°C)
DIESEL	128	265	40–280	184.5
HOME	210	297	108–498	274.2
JOME	146	334	140–490	277.3
JOME+HOME	167	267	126–403	191.9 and 245.8

**TABLE 4** Ignition, burnout temperature, DTG<sub>max</sub>, DTG<sub>mean</sub>, and  $T_{max}$  of biodiesels.

Sample	Ignition temperature, $T_i$ (°C)	Burnout temperature, $T_b$ (°C)	DTG <sub>max</sub>	DTG <sub>mean</sub>
DIESEL	128	283.24	7.92	2.43
HOME	278	445.96	13.46	2.69
JOME	220	470.02	8.44	2.09
HOME+JOME	126	360.28	13.28	2.784

**TABLE 5** Combustion characteristics of biodiesels.

Sample	Ignition index, $D_i \times 10^{-4}$ (wt % min <sup>-1</sup> °C <sup>-2</sup> )	Burnout index, $D_b \times 10^{-6}$ (wt % min <sup>-1</sup> °C <sup>-3</sup> )	Combustion index parameter, $S \times 10^{-6}$ (wt % min <sup>-2</sup> °C <sup>-3</sup> )	Intensity of combustion ( $H_i$ )
DIESEL	3.35	3.35	41.6	0.467
HOME	1.77	4.025	82.28	0.321
JOME	1.43	6.87	77.74	0.591
HOME+JOME	5.49	5.722	64.6	0.379

JOME, and equally mixed HOME and JOME biodiesel. The broader DTG curve of diesel is due to numerous organic compounds during decomposition.<sup>50,51</sup> Table 3 gives the maximum decomposition temperature for diesel, JOME, HOME, and equally mixed JOME and HOME biodiesel. The decomposition reaction temperature slowed down from 300°C for diesel. For HOME, JOME, and equally mixed JOME and HOME biodiesel, the reaction becomes inactive beyond 360, 390, and 275°C, respectively. DTG curve for mixed biodiesel confirmed rapid combustion with reduced peak temperature. JOME indicated low onset temperature and high volatility. The high peak temperature observed in the DTG curves suggests a lower reactivity of the fuels. Similar findings have been reported by Concone et al.<sup>56</sup> for the blends of Sugar cane biodiesel and diesel. JOME indicated less reactive when compared to HOME and mixed biodiesel (JOME+HOME). Mixed biodiesel (JOME+HOME) represented low decomposition temperature and better reaction region temperature.<sup>57,58</sup>

Table 4 gives ignition temperature ( $T_i$ ), burnout temperature ( $T_b$ ), DTG<sub>max</sub>, and DTG<sub>mean</sub>. Table 5 presents the combustion characteristics of biodiesels. Theoretically, the higher value of the ignition index infers the fuel to be enriched with higher volatile matter content, which is easily ignitable, as observed by Aich et al.<sup>43</sup> The burnout index provides the trend of the TG curve from the ignition point to the maximum rate of weight loss point (98%). High burnout index indicates better combustion reactivity.<sup>43</sup> Significant mass degradation of HOME in the third stage leads to a high combustion index. JOME decomposition involved high mass degradation in the third

stage and possessed high combustion index.<sup>59</sup> Mixed biodiesel exhibited a low end-set reaction temperature of 403.3°C and a low offset temperature compared to pure biodiesel. Hence, the low combustion index of mixed biodiesel possessed maximum decomposition at 191.9 and 245.8°C. High combustion index indicates a good combustion performance. A similar trend is noticed in the studies of Tang et al.<sup>60</sup>

## 4 | CONCLUSIONS

Thermal analysis techniques such as TGA and DSC are valuable methods for evaluating the thermal stability and combustion behavior of biodiesel and its derivatives. These techniques can provide insight into the stability of samples, which is beneficial for improving storage conditions before subjecting them to engine testing. Additionally, when blending biodiesel with diesel, the resulting sample may exhibit unique properties that can be better understood through thermal analysis. This article examines the thermal characteristics of diesel and HOME, JOME, and equally mixed HOME, and JOME biodiesel by performing TG-DSC analysis in air. Biodiesels showed three phases of decomposition. The stability of biodiesel depends on fatty acids composition; high content of unsaturated fatty acids (susceptible to oxidative degradation). From TG curves, the stability of samples is in the following order JOME, HOME, equally mixed JOME and HOME, and diesel. High content of oleic acid and linoleic acid in biodiesel

structure causes sensitivity to oxidation. Oleic and linoleic acid contents in JOME are 41.8% and 32.2%, whereas 46% and 27.1% in HOME. Mixed biodiesel represents low onset and offsets temperature and high volatility resembling diesel characteristics with improved properties. The peak temperature of combustion, enthalpy, ignition temperature, and burnout temperature for mixed biodiesel was found to be comparable with diesel. The ignition index of mixed biodiesel is 61% high when compared to diesel. The burnout index for mixed biodiesel is 58.54% high when compared to diesel. The burnout index for mixed biodiesel is 29.7% high when compared to HOME and 20% low when compared to JOME. The combustion index for mixed biodiesel is 36% high when compared to diesel, which follows the trend of TG-DSC analysis results. High mass degradation in the second stage indicates a high combustion index. Major mass degradation occurred in the second stage (combustion stage) for JOME and HOME. Therefore, they exhibited high combustion index when compared to diesel and mixed biodiesel. However, in overall efficiency, mixed biodiesel has a better intensity of combustion when compared to JOME and HOME. The combustion process is expected to occur smoothly and efficiently. High combustion index results in hard burning in the engine. Mixed biodiesel can be used as an alternative fuel for combustion applications. Future research efforts should focus on conducting TG-DSC experiments to investigate the thermal properties of biodiesels at different heating rates under nitrogen, argon, and oxygen environments.

## NOMENCLATURE

B-20	biodiesel 20%, diesel 80%.
DSC	differential scanning calorimetry
FAME	fatty acid methyl ester
FTIR	Fourier transform infrared spectrum
HOME	honge oil methyl ester
JOME	Jatropha oil Methyl Ester
TG-DTG	thermogravimetry-derivative thermogravimetry

## AUTHOR CONTRIBUTIONS

**Vinay Atgur:** Conceptualization, data curation, formal analysis, investigation, methodology, writing – original draft, writing – review & editing. **G. Manavendra:** Investigation, methodology, supervision, writing – original draft. **B. Nageswara Rao:** Formal analysis methodology, supervision, writing – review & editing. **Ibham Veza:** Resources, writing – review & editing. **I. M. Rizwanul Fattah:** Conceptualization, project administration, writing – original draft, writing – review & editing. All authors have read and approved the final manuscript.

## ACKNOWLEDGMENTS

The authors would like to acknowledge the Sophisticated Analytic instrumentation facility centre, the Indian Institute of Technology, Madras, for providing the testing facilities. Open access publishing facilitated by University of Technology Sydney, as part of the Wiley – University of Technology Sydney agreement via the Council of Australian University Librarians.

## FUNDING INFORMATION

This research was funded by University of Technology Sydney through Strategic Research Support funding with grant number (2200034).

## DATA AVAILABILITY STATEMENT

The data that support the findings of this study are available from the corresponding author upon reasonable request.

## ORCID

I. M. Rizwanul Fattah  <https://orcid.org/0000-0003-4170-4074>

## REFERENCES

- Ejaz A, Babar H, Ali HM, et al. Concentrated photovoltaics as light harvesters: outlook, recent progress, and challenges. *Sustain Energy Technol Assessments*. 2021;46:46101199. doi:10.1016/j.seta.2021.101199
- Manaf ISA, Embong NH, Khazaai SNM, et al. A review for key challenges of the development of biodiesel industry. *Energy Convers Manage*. 2019;185:508-517. doi:10.1016/j.enconman.2019.02.019
- Sadeghinezhad E, Kazi SN, Sadeghinejad F, et al. A comprehensive literature review of bio-fuel performance in internal combustion engine and relevant costs involvement. *Renew Sustain Energy Rev*. 2014;30:29-44. doi:10.1016/j.rser.2013.09.022
- Atgur V, Manavendra G, Desai GP, Nageswara RB. Thermogravimetry and calorimetric evaluation of honge oil methyl ester and its B-20 blend. *Clean Eng Technol*. 2022;6:100367. doi:10.1016/j.clet.2021.100367
- Atgur V, Manavendra G, Desai GP, Nageswara RB. Thermal characterisation of dairy washed scum methyl ester and its b-20 blend for combustion applications. *Int J Ambient Energy*. 2022;43(1):4433-4443. doi:10.1080/01430750.2021.1909651
- Ramkumar S, Kirubakaran V. Biodiesel from vegetable oil as alternate fuel for C.I engine and feasibility study of thermal cracking: a critical review. *Energy Convers Manage*. 2016;118:155-169. doi:10.1016/j.enconman.2016.03.071
- Rajasekar E, Selvi S. Review of combustion characteristics of CI engines fueled with biodiesel. *Renew Sustain Energy Rev*. 2014;35:390-399. doi:10.1016/j.rser.2014.04.006
- Banapurmath NR, Tewari PG, Hosmath RS. Combustion and emission characteristics of a direct injection, compression-ignition engine when operated on Honge oil, HOME and blends of HOME and diesel. *Int J Sustain Eng*. 2008;1(2):80-93. doi:10.1080/19397030802221265
- Lee XJ, Ong HC, Gao W, et al. Solid biofuel production from spent coffee ground wastes: process optimisation, characterisation and kinetic studies. *Fuel*. 2021;292:120309. doi:10.1016/j.fuel.2021.120309
- Vossoughi S, El-Shoubary YM. Kinetics of liquid hydrocarbon combustion using the DSC technique. *Thermochimica Acta*. 1990;157(1):37-44. doi:10.1016/0040-6031(90)80004-1
- Rahmanian B, Safaei MR, Kazi SN, Ahmadi G, Oztop HF, Vafai K. Investigation of pollutant reduction by simulation of turbulent non-premixed pulverized coal combustion. *Appl Therm Eng*. 2014;73(1):1222-1235. doi:10.1016/j.applthermaleng.2014.09.016
- Bilgin A, Gulum M. Effects of various transesterification parameters on the some fuel properties of hazelnut oil methyl ester. *Energy Procedia*. 2018;147:54-62. doi:10.1016/j.egypro.2018.07.033
- Gulum M, Bilgin A. Measurement and prediction of density and viscosity of different diesel-vegetable oil binary blends. *Environ Clim Technol*. 2019;23(1):214-228. doi:10.2478/rtulect-2019-0014
- Soudagar MEM, Mujtaba MA, Safaei MR, et al. Effect of Sr@ZnO nanoparticles and Ricinus communis biodiesel-diesel fuel blends on



- modified CRDI diesel engine characteristics. *Energy*. 2021;215:119094. doi:[10.1016/j.energy.2020.119094](https://doi.org/10.1016/j.energy.2020.119094)
15. Mofijur M, Siddiki SYA, Shuvho MBA, et al. Effect of nanocatalysts on the transesterification reaction of first, second and third generation biodiesel sources - a mini-review. *Chemosphere*. 2021;270:270128642. doi:[10.1016/j.chemosphere.2020.128642](https://doi.org/10.1016/j.chemosphere.2020.128642)
  16. Razaq L, Mujtaba MA, Soudagar MEM, et al. Engine performance and emission characteristics of palm biodiesel blends with graphene oxide nanoplatelets and dimethyl carbonate additives. *J Environ Manage*. 2021;282:111917. doi:[10.1016/j.jenvman.2020.111917](https://doi.org/10.1016/j.jenvman.2020.111917)
  17. Fattah IMR, Masjuki HH, Kalam MA, et al. Effect of antioxidants on oxidation stability of biodiesel derived from vegetable and animal based feedstocks. *Renew Sustain Energy Rev*. 2014;30:356-370. doi:[10.1016/j.rser.2013.10.026](https://doi.org/10.1016/j.rser.2013.10.026)
  18. Hoang AT, Ong HC, Fattah IMR, et al. Progress on the lignocellulosic biomass pyrolysis for biofuel production toward environmental sustainability. *Fuel Process Technol*. 2021;223:106997. doi:[10.1016/j.fuproc.2021.106997](https://doi.org/10.1016/j.fuproc.2021.106997)
  19. Mofijur M, Masjuki HH, Kalam MA, Atabani AE, Fattah IMR, Mobarak HM. Comparative evaluation of performance and emission characteristics of *Moringa oleifera* and Palm oil based biodiesel in a diesel engine. *Indus Crops Products*. 2014;53:78-84. doi:[10.1016/j.indcrop.2013.12.011](https://doi.org/10.1016/j.indcrop.2013.12.011)
  20. Lai JYW, Lin KC, Violi A. Biodiesel combustion: advances in chemical kinetic modeling. *Prog Energy Combust Sci*. 2011;37(1):1-14. doi:[10.1016/j.pecc.2010.03.001](https://doi.org/10.1016/j.pecc.2010.03.001)
  21. K ok MV. Thermal analysis applications In fossil fuel science. Literature survey. *J Therm Anal Calorim*. 2002;68(3):1061-1077. doi:[10.1023/A:1016119428815](https://doi.org/10.1023/A:1016119428815)
  22. Lamprecht I. Chapter 4 - combustion calorimetry. In: Kemp RB, ed. *Handbook of thermal analysis and calorimetry*. Elsevier Science B.V.; 1999:175-218.
  23. Longanesi L, Pereira AP, Johnston N, Chuck CJ. Oxidative stability of biodiesel: recent insights. *Biofuels Bioprod Biorefin*. 2022;16(1):265-289. doi:[10.1002/bbb.2306](https://doi.org/10.1002/bbb.2306)
  24. Chong KJ, Bridgwater AV. Fast pyrolysis oil fuel blend for marine vessels. *Environ Prog Sustain Energy*. 2017;36(3):677-684. doi:[10.1002/ep.12402](https://doi.org/10.1002/ep.12402)
  25. Wategave SP, Banapurmath NR, Sawant MS, et al. Clean combustion and emissions strategy using reactivity controlled compression ignition (RCCI) mode engine powered with CNG-Karanja biodiesel. *J Taiwan Inst Chem Eng*. 2021;124:116-131. doi:[10.1016/j.jtice.2021.04.055](https://doi.org/10.1016/j.jtice.2021.04.055)
  26. Sanjeevannavar MB, Banapurmath NR, Soudagar MEM, et al. Performance indicators for the optimal BTE of biodiesels with additives through engine testing by the Taguchi approach. *Chemosphere*. 2022;288:132450. doi:[10.1016/j.chemosphere.2021.132450](https://doi.org/10.1016/j.chemosphere.2021.132450)
  27. El-Sayed SA, Ismail MA, Mostafa ME. Thermal decomposition and combustion characteristics of biomass materials using TG/DTG at different high heating rates and sizes in the air. *Environ Prog Sustain Energy*. 2019;38(4):13124. doi:[10.1002/ep.13124](https://doi.org/10.1002/ep.13124)
  28. Kotaiah Naik D, Shuaib Ahmed M, Aniya V, Parthasarathy R, Satyavathi B. Torrefaction assessment and kinetics of deoiled Karanja seed cake. *Environ Prog Sustain Energy*. 2017;36(3):758-765. doi:[10.1002/ep.12534](https://doi.org/10.1002/ep.12534)
  29. Riayatsyah TMI, Sebayang AH, Silitonga AS, et al. Current progress of *Jatropha curcas* commoditisation as biodiesel feedstock: a comprehensive review. *Review*. *Front Energy Res*. 2022;1-19. doi:[10.3389/fenrg.2021.815416](https://doi.org/10.3389/fenrg.2021.815416)
  30. Tao J, Penmetza VK, Steele PH. Addition of gaseous olefin to produce boiler fuel and stability studies. *Environ Prog Sustain Energy*. 2015;34(3):933-941. doi:[10.1002/ep.12067](https://doi.org/10.1002/ep.12067)
  31. Atgur V, Manavendra G, Banapurmath NR, et al. Essence of thermal analysis to assess biodiesel combustion performance. *Energies*. 2022;15(18):6622.
  32. Atgur V, Manavendra G, Desai GP, et al. Thermogravimetric and combustion efficiency analysis of *Jatropha curcas* biodiesel and its derivatives. *Biofuels*. 2022;13(9):1069-1079. doi:[10.1080/17597269.2022.2090136](https://doi.org/10.1080/17597269.2022.2090136)
  33. Volli V, Purkait MK. Physico-chemical properties and thermal degradation studies of commercial oils in nitrogen atmosphere. *Fuel*. 2014;117:1010-1019. doi:[10.1016/j.fuel.2013.10.021](https://doi.org/10.1016/j.fuel.2013.10.021)
  34. Farias RMC, Concei ao MM, Candeia RA, Silva MCD, Fernandes VJ, Souza AG. Evaluation of the thermal stability of biodiesel blends of castor oil and passion fruit. *J Therm Anal Calorim*. 2011;106(3):651-655. doi:[10.1007/s10973-011-1566-x](https://doi.org/10.1007/s10973-011-1566-x)
  35. Santos AGD, Caldeira VPS, Souza LD, Oliveira DS, Araujo AS, Luz GE. Study of the thermal stability by thermogravimetry for oil, biodiesel and blend (B10) of different oilseeds. *J Therm Anal Calorim*. 2016;123(3):2021-2028. doi:[10.1007/s10973-015-4943-z](https://doi.org/10.1007/s10973-015-4943-z)
  36. Dwivedi G, Sharma MP. Experimental investigation on thermal stability of Pongamia biodiesel by thermogravimetric analysis. *Egypt J Petrol*. 2016;25(1):33-38. doi:[10.1016/j.ejpe.2015.06.008](https://doi.org/10.1016/j.ejpe.2015.06.008)
  37. Concei ao MM, Candeia RA, Silva FC, Bezerra AF, Fernandes VJ, Souza AG. Thermoanalytical characterization of castor oil biodiesel. *Renew Sustain Energy Rev*. 2007;11(5):964-975. doi:[10.1016/j.rser.2005.10.001](https://doi.org/10.1016/j.rser.2005.10.001)
  38. John CB, Solamalai AR, Jambulingam R, Balakrishnan D. Estimation of fuel properties and characterization of hemp biodiesel using spectroscopic techniques. *Energy Sources A Recov Utiliz Environ Eff*. 2020;1-18. doi:[10.1080/15567036.2020.1842559](https://doi.org/10.1080/15567036.2020.1842559)
  39. Wnorowska J, Ciukaj S, Kalisz S. Thermogravimetric analysis of solid biofuels with additive under air atmosphere. *Energies*. 2021;14(8):2257.
  40. Banapurmath NR, Tewari PG, Hosmath RS. Performance and emission characteristics of a DI compression ignition engine operated on Honge, *Jatropha* and sesame oil methyl esters. *Renew Energy*. 2008;33(9):1982-1988. doi:[10.1016/j.renene.2007.11.012](https://doi.org/10.1016/j.renene.2007.11.012)
  41. Deepanraj B, Srinivas M, Arun N, Sankaranarayanan G, Abdul SP. Comparison of *jatropha* and *Karanja* biofuels on their combustion characteristics. *Int J Green Energy*. 2017;14(15):1231-1237. doi:[10.1080/15435075.2017.1328420](https://doi.org/10.1080/15435075.2017.1328420)
  42. Soudagar MEM, Khan HM, Khan TMY, et al. Experimental analysis of engine performance and exhaust pollutant on a single-cylinder diesel engine operated using *Moringa oleifera* biodiesel. *Appl Sci*. 2021;11(15):7071.
  43. Aich S, Behera D, Nandi BK, Bhattacharya S. Relationship between proximate analysis parameters and combustion behaviour of high ash Indian coal. *Int J Coal Sci Technol*. 2020;7(4):766-777. doi:[10.1007/s40789-020-00312-5](https://doi.org/10.1007/s40789-020-00312-5)
  44. Swathi D, Gopa B, Rao P, Raju G. Optimization of *jatropha* methyl ester and study of its physico-chemical properties using GC-MS and FT-IR analysis. *Austin Chem Eng*. 2016;3(2):1027.
  45. Almazrouei M, Janajreh I. Thermogravimetric study of the combustion characteristics of biodiesel and petroleum diesel. *J Therm Anal Calorim*. 2019;136(2):925-935. doi:[10.1007/s10973-018-7717-6](https://doi.org/10.1007/s10973-018-7717-6)
  46. Dantas MB, Albuquerque AR, Soledade LEB, et al. Biodiesel from soybean oil, castor oil and their blends. *J Therm Anal Calorim*. 2011;106(2):607-611. doi:[10.1007/s10973-011-1410-3](https://doi.org/10.1007/s10973-011-1410-3)
  47. Mohammed MN, Atabani AE, Uguz G, Lay C-H, Kumar G, Al-Samarrae RR. Characterization of hemp (*Cannabis sativa* L.) biodiesel blends with euro diesel, butanol and diethyl ether using FT-IR, UV-vis, TGA and DSC techniques. *Waste Biomass Valoriz*. 2020;11(3):1097-1113. doi:[10.1007/s12649-018-0340-8](https://doi.org/10.1007/s12649-018-0340-8)
  48. Chabane S, Benziane M, Khimeche K, Trache D, Didaoui S, Yagoubi N. Low-temperature behavior of diesel/biodiesel blends. *J Therm Anal Calorim*. 2018;131(2):1615-1624. doi:[10.1007/s10973-017-6614-8](https://doi.org/10.1007/s10973-017-6614-8)

49. Nicolau CL, Klein ANV, Silva CAA, et al. Thermal properties of the blends of methyl and ethyl esters prepared from babassu and soybean oils. *J Braz Chem Soc.* 2018;29(8):1672-1679.
50. Freire LMS, Bicudo TC, Rosenhaim R, et al. Thermal investigation of oil and biodiesel from *Jatropha curcas* L. *J Therm Anal Calorim.* 2009; 96(3):1029-1033. doi:10.1007/s10973-009-0055-y
51. Jain S, Sharma MP. Thermal stability of biodiesel and its blends: a review. *Renew Sustain Energy Rev.* 2011;15(1):438-448. doi:10.1016/j.rser.2010.08.022
52. Singh R, Padhi S. Characterisation of jatropha oil for the preparation of biodiesel. *Nat Prod Radiance.* 2009;8(2):127-132.
53. Jain S, Sharma MP. Correlation development between the oxidation and thermal stability of biodiesel. *Fuel.* 2012;102:354-358. doi:10.1016/j.fuel.2012.06.110
54. Soto F, Alves M, Valdés JC, et al. The determination of the activation energy of diesel and biodiesel fuels and the analysis of engine performance and soot emissions. *Fuel Process Technol.* 2018;174:69-77. doi:10.1016/j.fuproc.2018.02.008
55. Peer MS, Kasimani R, Rajamohan S, Ramakrishnan P. Experimental evaluation on oxidation stability of biodiesel/diesel blends with alcohol addition by rancimat instrument and FTIR spectroscopy. *J Mech Sci Technol.* 2017;31(1):455-463. doi:10.1007/s12206-016-1248-5
56. Conconi CC, Crnkovic PM. Thermal behavior of renewable diesel from sugar cane, biodiesel, fossil diesel and their blends. *Fuel Process Technol.* 2013;114:6-11. doi:10.1016/j.fuproc.2013.03.037
57. Singh Chouhan AP, Singh N, Sarma AK. A comparative analysis of kinetic parameters from TGDTA of *Jatropha curcas* oil, biodiesel, petroleum diesel and B50 using different methods. *Fuel.* 2013;109: 217-224. doi:10.1016/j.fuel.2012.12.059
58. Li H, Liu F, Zhou S, Liu J, Wu Z. Thermal degradation characteristics of rapeseed biodiesel and its blends with petroleum diesel. *Heat Transf Eng.* 2020;41(9-10):896-904. doi:10.1080/01457632.2019.1576823
59. Ren X, Meng J, Moore AM, Chang J, Gou J, Park S. Thermogravimetric investigation on the degradation properties and combustion performance of bio-oils. *Bioresour Technol.* 2014;152:267-274. doi:10.1016/j.biortech.2013.11.028
60. Tang L, Xiao J, Mao Q, et al. Thermogravimetric analysis of the combustion characteristics and combustion kinetics of coals subjected to different chemical demineralization processes. *ACS Omega.* 2022; 7(16):13998-14008. doi:10.1021/acsomega.2c00522

**How to cite this article:** Atgur V, Manavendra G, Rao BN, Veza I, Fattah IMR. Thermal and combustion characteristics of honge, jatropha, and honge-jatropha mixed biodiesels. *Environ Prog Sustainable Energy.* 2023:e14199. doi:10.1002/ep.14199